The correct citation for this paper is:

Moallem, E., Padhmanabhan, S., Cremaschi, L., and Fisher, D.E. (2010) Experimental Study of Onset and Growth of Frost on Outdoor Coils of Air-Source Heat Pumps. Proceedings of ASME-ATI-UIT. Conference on Thermal and Environmental Issues in Energy Systems May 2010. Sorrento, Italy.

ASME-ATI-UIT 2010 Conference on Thermal and Environmental Issues in Energy Systems
16 – 19 May, 2010, Sorrento, Italy

EXPERIMENTAL STUDY OF ONSET AND GROWTH OF FROST ON OUTDOOR COILS OF AIR-SOURCE HEAT PUMP SYSTEMS

Ehsan Moallem*, Sankar Padhmanabhan*, Lorenzo Cremaschi*, and Daniel E. Fisher*

* School of Mechanical & Aerospace Engineering, Oklahoma State University, Stillwater, OK, 74078, USA
moallem@okstate.edu

ABSTRACT

This paper addresses frost growth on fin-and-tube and microchannel heat exchangers used in air-source heat pump systems. Experimental data of local frost weight and frost thickness are presented for heat exchangers operating in actual transient frosting conditions. Frost weight growth rate was directly measured on small-scale laboratory coils that were anchored to a precision scale and local frost thickness was recorded simultaneously at various sections of the heat exchangers. Operating conditions were maintained by installing the coils in a laboratory test facility that replicated the environment to which outdoor coils are exposed to. The effects of fin surface temperature and air relative humidity on the frost deposition time and frost growth rate were experimentally investigated. It was found that the increase of frost thickness depends on the location of the fin with respect to the inlet refrigerant header, that is, on the local fin surface temperature. It was also measured that microchannel coils frost faster than fin and tube coil in the same operating conditions and the main reasons were attributed to lower fin surface temperature and fin geometry.

INTRODUCTION

Air source heat pump systems are used for heating and cooling buildings all year around. They are energy efficient, compact and have low installation cost. An air source heat pump exchanges heat directly from the indoor environment to the outdoor ambient air, and during winter operation, the outdoor coil might accumulate frost on its surface. Defrost cycles are periodically executed in between the heating time to melt the ice, drain the water from the outdoor coil, and free its surface from accumulated frost before the heating service could start again. Heat pumps with microchannel type outdoor evaporators defrost more often than fin-and-tube heat pump units, operating under similar conditions, and the overall heating seasonal performance factor is in most cases are lower than conventional fin-and-tube heat exchangers [1, 2]. Because frequent defrost cycles penalize the seasonal energy efficiency, it is crucial to understand characteristics of frost formation on outdoor coils and design heat exchangers that would minimize, if not eliminate, defrost cycles.

The fundamental understanding of the heat and mass transfer characteristics of coils during frosting and defrosting transient periods are still not well-known. Most of the results are based on a limited range of experimental tests in which fin design effects are difficult to isolate and quantify [3-5]. Other studies focused on simplified geometries, such as flat plates or channel flows between parallel flat plates [6, 7]. The complexity of the phenomena makes the theoretical analysis problematic, and increases the difficulty in accurately measuring the influence of fin surface temperature, fin geometry, and fin surface energy on frost growth [8, 9].

There are several parameters that affect frost formation on outdoor coils, such as air velocity, air humidity, air temperature, cold surface temperature, surface energy, and fin-base surface microscopic characteristics [10]. Frost thickness influences the heat transfer resistance and causes heating capacity degradation. Various techniques have been used in the literature to measure frost thickness: for example mechanical methods with micrometers by Lee et al. [11], Na et al. [12] and Fossa et al. [13]; optical or laser methods by Kennedy et al. [14] and Chen et al. [15]; and imagery analysis by Xia et al. [16]. With mechanical measurements methods, the accurate measurements of frost build up might not be possible due to the fact that it is necessary to stop the experiment to obtain the measurement or the micrometer might interrupt local air stream and hinder the onset of frost growth. Researchers reported laser beam methods to be impractical in most cases due to high roughness of the frost surface [12]. Imagery analysis proved to be successful in measuring the frost thickness with good accuracy but the data reduction is a very lengthy process. In the literature, the frost thickness was mostly measured at one location of the coil, which is a reasonable trade off only if the frost growth is uniform throughout the coil. Unfortunately this is not always the case even for laboratory tests.

Different methods for measuring the frost weight were proposed in the literature. The direct weight measurements using precision scales in air flow wind tunnels or load cells in psychrometric chambers generally yield more accurate results. Scraping the frost from the coil and measuring its weight at the end of the test [17], or melting the frost and weighting the water condensate [18, 19], or adopting sophisticated scale mechanism to balance the frost weight [20] are examples used in past studies but are not necessarily suitable to determine the onset of frost nucleation and the instantaneous frost growth rate in compact coils. A successful method to measure frost growth is described in Verma et al. [21] and more recently by Xia et al. [5]. The authors proposed to weigh directly small

coil samples hung freely from a digital scale and compare the final weight with the amount of condensate. Their approach is promising but particular care must be taken to eliminate the friction, air drag and lift effects on the coil, which ultimately is immersed freely in an air stream. Residual stress in the connecting refrigerant lines and flexible duct seals must also be carefully evaluated before the data reduction of the frost weight. When the amount of frost accumulated is small, the uncertainty in the measurements due to these effects could skew the data.

From the literature review it appears that most of the frost measurements were conducted on simplified geometries with the assumption of uniform onset of frost growth. There is little or no information about experimental techniques to characterize transient, heterogeneous nucleation and frost growth on fin-and-tube and folded fins microchannel heat exchangers during their operation as outdoor evaporators. This paper describes an innovative technique to measure the onset of frost nucleation and procedures to determine the frost growth rates on fin-and-tube and microchannel heat exchangers used in air-source heat pump systems. Experimental data of frost weight, frost thickness, and frost distribution are presented for the heat exchanger summarized in Table 1. The fin and tube coil consisted of 12 horizontal tubes of about 10 mm inner diameter with vertical flat fins. Figure 1 shows the fin and tube test coil mounted in the wind tunnel. The frontal area was about 0.305m by 0.305m (approximately 1ft by 1ft) and the refrigerant flowed from the left to the right of Figure 1 in a single pass. For clarity, no insulation is shown in Figure 1 around the vertical headers and the flexible hoses, but during the experiments both headers and inlet and outlet flexible hoses were heavily insulated.

Table 1. Fin & Tube Heat Exchanger Geometries

Parameter	Value
No. of Rows	1
Finned Length (mm)	305
Coil (Finned) Heaight (mm)	305
No. of Tubes	12
Fin (Coil) Depth (mm)	22.1
Fin Distance (mm)	1.59
Fin Thickness (mm)	0.10
Tube Outer Diameter (Riffle Expanded) (mm)	10.67
Tube Inner Diameter (Riffle Expanded) (mm)	10.06

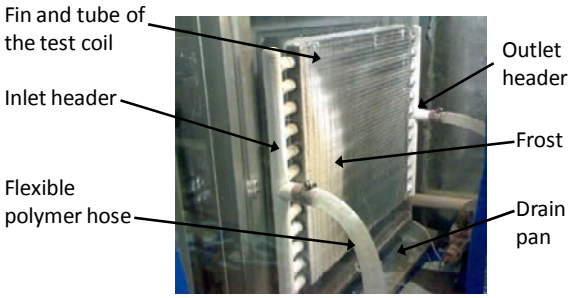

Figure 1: Image of the fin-and-tube test coil under frosting inside the low temperature air wind tunnel

A microchannel coil with similar frontal area of 0.305m×0.305m was also tested in the facility and its frosting characteristics were compared with the fin and tube coil. The microchannel coil consisted of 27 vertical tubes with 10 ports in each tube, and louvered folded fins. The distanced between the tubes was about 11mm and the fin spacing was 1.3mm. Refrigerant flowed from the bottom to the top of the microchannel coil in a single pass.

EXPERIMENTAL SETUP

In the present study, the test coils were set inside a controlled low temperature air wind tunnel facility, which is schematically shown in Figure 2. The test coil is exposed to controlled frosting conditions and is shown as component 5 in Figure 2. The low temperature air wind tunnel consisted of a closed duct system containing a centrifugal fan, a large refrigeration coil, an electrical heater, turning vanes, nozzles for flow measurements, humidifiers, thermocouples, pressure reading tubes, dew point meters and a digital scale. Air enters the test coil at 1.7°C dry bulb and 0.6°C wet bulb temperatures (35/33°F db/wb). This yields an entering relative humidity of about 82% during the experiments. The approaching air velocity is controlled by a variable speed fan and ranged from 0.7 to 1.5 m/s . These inlet conditions were controlled within a precision specified in the standard AHRI 210 for heat pump system performance rating [22]. A variable frequency inverter drove the fan using a PID controller. Three ultrasonic humidifiers were installed at the top section inside the wind tunnel to guarantee sufficient time for mixing and to achieve the desired humidity in the air stream. The cooling load of the tunnel was met by a large refrigeration coil connected to a low temperature chiller. The temperature and flow rate of the refrigeration coil were controlled by PID controllers and metering valves. Air leaving the refrigeration coil was heated by a 1.4 kW variable power electrical heater, whose capacity was adjusted to accurately set the air temperature approaching the test coil.

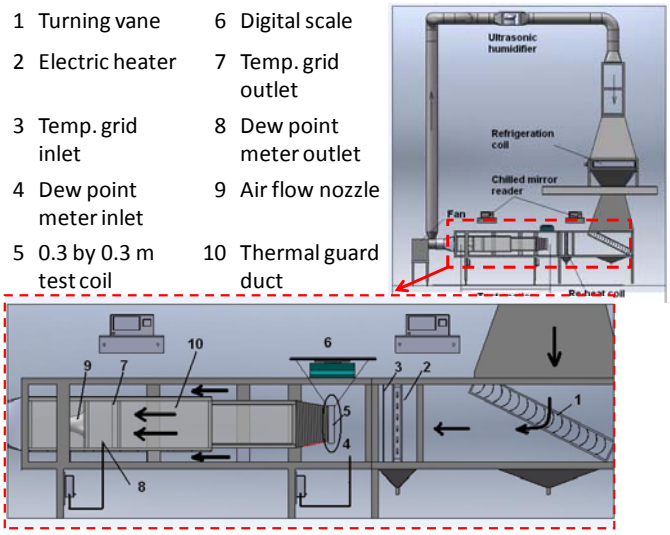

Figure 2: Schematic of the air wind tunnel for low temperature frosting experiments

A nozzle was mounted downstream of the test section to measure the air mass flow rate according to ASHRAE 41.2 [23]. Extra care was taken to improve the heat balance and minimize the effect of parasitic heat gains from the surroundings to the test coil. A dual concentric square duct tunnel was designed for this purpose, and it is shown in the

bottom schematic of Figure 2. While the main air flow circulated through the inner tunnel (component 10 in Figure 2), a fraction of the air flow is bypassed between the inner and the outer tunnel. This air gap acts as a guard space for the inner tunnel and results in near-adiabatic boundary conditions for the air flowing in the inner tunnel. The flow nozzle and temperature sensors were mounted inside the inner tunnel. Sixteen calibrated T-Type copper constantan thermocouples (4×4 grid) and one calibrated RTD were used to calculate the average air temperature and the air temperature uniformity at the front section of the test coil. After the test coil a similar 3×3 thermocouple grid measured the coil outlet temperature. The inlet and outlet grids are indicated in Figure 2 as comp. 3 and 7, respectively. The air pressure drop across the coil was measured by a pressure difference transducer and air humidity was measured using two chilled mirror dew point meters before and after the coil test section. The accuracy, calibration, and control tolerance of the instrumentation are summarized in Table 2.

Table 2. Measurement devices, set points, accuracies & test tolerances

Parameter measured	Measuring device	Calibration	Set point	Accur.	Control toleranc.
Air temp. (Dry bulb)	Thermocouple (Grid) + RTD	In situ*	1.67°C (35°F)	0.15°C	±0.56°C (ARI)
Air temp. (Wet bulb)	Chilled mirror dew point meter	Manufac.	0.56°C (33°F)	0.1°C	±0.28°C (ARI)
Fluid temp.	RTD	In situ*	-18, -23, -26°C	0.1°C	±0.25°C
Fluid mass flow rate	Coriolis mass flow meter	Manufac.	0.345 (kg/s)	±0.1%	0.0005 (kg/s)
Air volum. flow rate	ASHRAE Nozzle	In situ	0.07, 0.09, 0.13 m³/s	±2.3%	0.0014 m³/s
Air press.	Manometer	In situ	NA	2.5 (Pa)	NA

* NesLab Instruments Inc. constant temperature bath chiller model RTE-140 was used.

Controls and Instrumentations

A nominal 2.5 ton customized packaged water cooled reciprocating chiller was used to provide cooling requirements to the test facility. A secondary refrigeration loop was built to accurately set the conditions to the test coil. The secondary loop consisted of cold and hot storage tanks, a Coriolis flow meter, two high precision platinum RTDs and a variable speed pump. It circulated a solution of water and Ethylene Glycol 50/50 volume and it controlled the inlet refrigerant temperature to the test coils in the range from -26 to 0°C during the frosting tests and with a constant flow rate of 0.345 kg/s. The secondary loop was capable of quickly switching the entering refrigerant temperature from cold to hot by opening a valve from the hot tank and bypassing the cold tank. This process mimicked the defrost cycle of a heat pump. Ethylene Glycol was maintained at about 20°C in the hot tank, and it was pumped to the test coils during the defrost periods.

All of readings from the thermocouples, pressure transducers and flow meters were recorded using a Fluke® 2680 data logging acquisition system with a scan rate of 4 seconds. Control boards PCI-DAC 6703 and PCI-DAS 6025 from Measurement Computing® were used to provide low voltage control signals. A program was written in the LabView® ver.8.5 software environment to calculate derived quantities, plot the data, and control the test facility. More details of the test facility are provided by Cai [24].

Frost Weight Measurements

Each test coil was suspended in the wind tunnel and hung from the digital scale (comp. 6 in Figure 2), which recorded the frost growth rate during the tests with a nominal accuracy of 0.2g. Four wires connected the top section of the test coil to the scale as shown in Figure 2. The 45 degree angle of attachment kept the test coil stable and, at the same time allowed it to move freely along the vertical direction. A very thin plastic film was installed loosely before and after the test coils to provide an air seal between the inner duct and the tunnel. Two flexible polymer hoses were used for the refrigerant connections; they were clamped between the secondary loop and the test coil refrigerant ports. Each flexible hose was about 1 meter long, and it was coiled one time around itself before it was connected to the port of the heat exchanger. This configuration eliminated any structural constraints to the vertical displacements of the test coil when frost accumulated on its surface.

In this study, the primary measurement of the frost mass accumulated on the fins was the weight increase of the coil during the test. Through a series of calibration tests, it was observed that the effects of air lift and drag on the test coil caused a systematic error in the measurements of the frost weight. To eliminate this error, the fan was periodically stopped 4 to 5 times for short intervals during each frosting experiment. Each pause was no longer than one minute and allowed the air in the tunnel to come to a rest. In the absence of forced air flow, the test coil was temporarily released from the effects of lift, drag, and static friction, and a new equilibrium position was achieved. Once the frost weight was sampled and recorded, the fan was started again and the test continued until the next pause. It should be noticed that only the air flow in the tunnel was interrupted while the refrigerant flow was run constantly during the entire experiment. An investigation was performed to check whether the sampling rates of the weight might affect the mode of growth for the frost. Tests at similar conditions were repeated several times using two different procedures. In one procedure, the fan was periodically stopped every 5 to 10 minutes to measure the free weight, and in the other procedure, the air flow rate was continuous. The final weight of frost was checked with the final weight of condensate from the coil and the difference in air humidity estimated from the dew point measurements. This was done to verify that the frost weight from the scale was in agreement with the other two methods. The final frost masses from the two tests were compared, and it was observed that although the readings from the scale when the air flow was continuous were always lower than the actual frost mass, once the fan was stopped at the end of the test, the final frost weight from both procedures were the same. As expected air pressure drop and frosting periods were similar for both procedures. A sensitivity study of the length of the pauses was also conducted and it was concluded that a one minute pause was optimal for sampling the weights. While longer pauses slightly increased the accuracy and repeatability of the weight measurements, they also affected the frost growth pattern.

Frost Thickness Measurements

A typical frost pattern for the fin and tube test coil is shown in Figure 1. The frost grows prevalently from the central tubes

and forms a curved profile that advances continuously from left to right. The frost thickness was captured by a high resolution short focus CCD (Charge-Coupled Device) camera, which included a 1 meter extended mini probe head. The probe tip of the CCD camera was installed at the front of the test coil and mounted on a programmable robotic arm connected to three stepper motors. Frost thickness was taken periodically every 3 minutes at four locations along the central tube of the coil. An anemometer was also installed near the CCD probe tip to qualitatively observe the local approaching air velocity. The images were processed after each experiment to obtain the frost thickness in each location. Estimates showed that the initial (dry) fin surface temperature was about 10 to 16°C higher than the temperature of the entering Ethylene Glycol. The authors attempted to attach thermocouples to the fins but the contact resistance was too high to provide a representative value of the fin surface temperature.

During the frosting period for the fin and tube coil, while it could be assumed that the frost thickness was quite uniform along the vertical direction of the coil, the front edge of the frost clearly advanced during the experiment from the inlet to the outlet. This was due to a high thermal entry length for the Ethylene Glycol solution flowing inside the 10mm diameter copper tube. A snapshot of this frosting process is shown in Figure 1. a. Four locations along the central horizontal tube were chosen as targets for the CCD camera and their distance from the refrigerant inlet header was 0.06, 0.12, 0.18 and 0.24m. During the experiments the camera moved in between these locations to capture the frost thickness at various time. An example of frost thickness measurment is shown Figure 3. The values of frost thickness was obtained by overlaying sequential photos of the frost and measuring the distance of the frost profile with respect to the dry fin surface edge. The frost thickness ranged between 0 and 0.76mm, which was half of the distance between two adjacent fins. The accuracy of the frost thickness measurements was about 0.03mm. Each image was analyzed using the iViewPC® ver. 5.0 software. Further details of the programmable robotic arms and camera controls are provided by Carroll et al. [25].

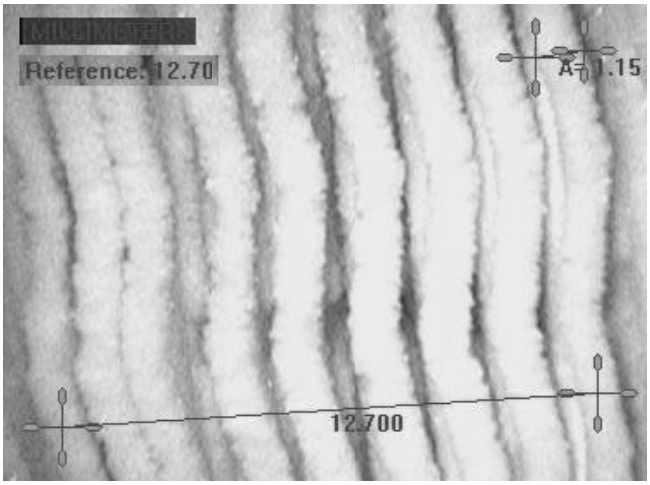

Figure 3: Example of frost thickness measurement on fins of the fin and tube heat exchanger

Uncertainty Analysis

The uncertainty in air volumetric flow rate was calculated to be less than ±2.3%. This uncertainty was calculated for 1.5 m/s entering air velocity, which was the maximum limit in the experiments. Other uncertainties for air db/wb temperatures, refrigerant temperature and flow rates are shown in Table 2. The uncertainty in total heat transfer rate was calculated to be within ±10% for the refrigerant side and around ±9% for air side. The heat balance error was well within 5% during dry heat transfer tests and increased to 10% for the initial periods of the wet and frost tests. Because of the transient nature of the experiments, the heat balance error increased to up to 20% in average and occasionally reached 30% at the end of the frost period. The authors believed that this deviation is due to transient heat conduction effects, thermal mass storage effects, and frost densification effects. Furthermore, the chilled mirror dew point meters provided inherently uncertain measurements when near to frosting conditions and they might lag the actual of water vapour removal from the air stream. From an analysis of the set up, hysteresis and from the extensive calibration and shakedown tests, the authors concluded than the frost weight could be measured with an accuracy of about ±10g.

RESULTS AND DISCUSSION

To evaluate the influence of each frost formation factor on the coil a series of experiments were conducted at various air and refrigerant conditions. All tests were conducted with the heat exchangers initially in dry surface conditions and at constant air temperature and air bulk velocity. The measured quantities are presented in normalized form with respect to the maximum value. Figure 4 shows the frost thickness at various location of the fin-and-tube test coil. Frost grows prevalently in between the fins along the *x*-direction, and the thickness is expressed in term of fraction of fin space covered by frost to the fin spacing of the fin and tube heat exchanger. Frost built up along the *x*- direction perpendicular to the air flow (in *y* direction) until the intersection of two frost layers of adjacent fins was reached. Frost blocked the air passage between the fins and, the air flow is continuously redistributed among the fins of the heat exchanger that offer the least resistance to the air path. When the air gap in between two fins is completely filled with frost, further densification of the frost occurs. Due to non uniform frost growth on the front area of the heat exchanger, the thickness was recorded for zones (1) to (4) of Figure 4. Estimates of the fin surface temperature revealed that the local fin temperature is the lowest at the inlet of zone (1) and increases up to about 6°C higher at the outlet of zone (4), even though the refrigerant temperature difference from the inlet to the outlet was only 1°C. This was consistent with visual observations of frost propagation from left to right side of the coil during the test. The frost nucleation time is delayed when moving from the inlet of zone (1) to the outlet of zone (4) and this phenomenon seems to suggest that the frost nucleation is quite sensitive to the local fin surface temperature rather than the refrigerant bulk temperature. After the initial delay, the frost growth rates in the four sections of the coil were similar.

Figure 5 shows the effect of entering refrigerant temperatures on the frost growth mass on the fin and tube coil. Each refrigerant temperature yielded a different fin surface temperature distribution, which was estimated in detail in [26]. During these tests the air entering speed was kept constant by adjusting the VFD power to the fan. The test was terminated when the air entering velocity dropped by more than 5% of the nominal (initial) value even with the maximum

fan power. The frost growth rate increases if the refrigerant temperature is lower as indicated in the initial slopes in Figure 5. The frost growth rate at -26°C refrigerant temperature was very high at the beginning of the test and a fairly fluffy, low density frost covered the entire frontal area of heat exchanger. Due to the excessive pressure drop across the frosted coil, the fan was not able to maintain the constant air velocity of 1m/s and the test was stopped at 45 minutes.

Figure 6 provides data of frost thickness versus entering air humidity. As expected, higher relative humidity had a significant effect on the frost growth rate. An increase of only 10% in the air relative humidity, that is, from 82% to 92%R.H., doubled the frost accumulation rate and the air-side pressure drop. The augmented moisture content in the air stream promoted early nucleation of frost and cause higher frost growth rates on the fins.

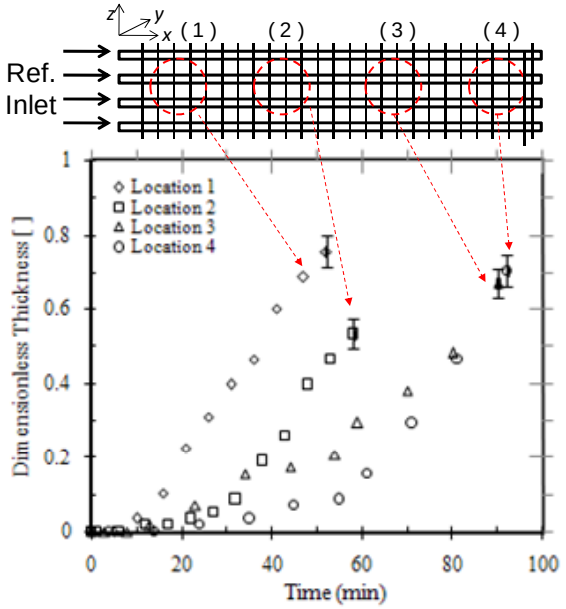

Figure 4: Frost formation in different locations of the fin and tube heat exchanger under constant air temperature (1.7ºC/0.6ºC db/wb 82% rel. hum. AHRI) and velocity (1.0m/s), constant refrigerant (ethylene glycol) temperature (-18ºC) and flow rate (0.345kg/s). Absolute error bars apply to all data points.

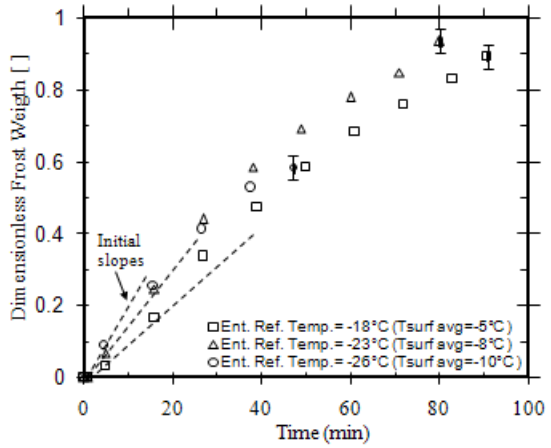

Figure 5: Effect of entering fluid temperature (eventually surface temperature) on weight of frost formation on fin and tube coil under constant air temperature (1.7ºC/0.6ºC db/wb AHRI) and velocity (1.0m/s), constant refrigerant (ethylene glycol) flow rate (0.345kg/s). Absolute error bars apply to all points.

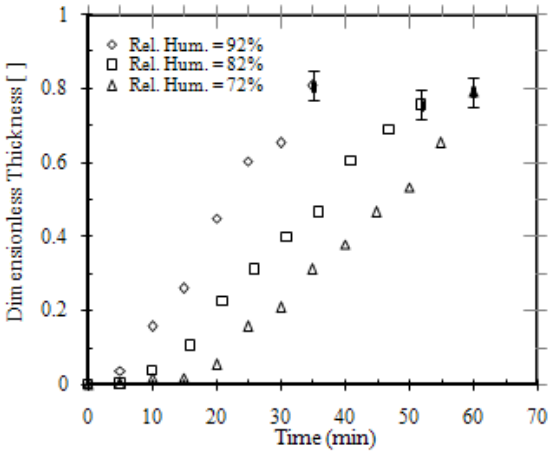

Figure 6: Effect of air humidity on frost formation on fin and tube coil under constant air temperature (1.7ºC db) and velocity (1.0m/s), constant refrigerant (ethylene glycol) temperature (-18 ºC) and flow rate (0.345kg/s). Absolute error bars apply to all points.

A comparison of frost weight between the fin and tube coil and the microchannel coil with similar cross sectional frontal area is provided in Figure 7. It is evident that the rate of frost growth on the microchannel coil was significantly higher than on the fin and tube coil. If the two coils shared similar entering refrigerant temperature (ERT), the frosting time was 90 minutes and 10 minutes for fin-and-tube and microchannel coil, respectively. However, the fin surface temperature for the microchannel coil with ERT of -18°C was estimated to be much lower than the one for the fin-and-tube coil. If the surface temperature for both coils ranged between -6 and -8°C, the data plotted in Figure **7** show that frosting time for the microchannel coil was about 40 minutes and still half of the time with respect to the frosting period of fin and tube coil operating at similar surface temperatures. Both coils experienced longer frosting periods when the fin temperature was increased and the microchannel coil seemed to pack frost in a shorter time due to its fin geometry.

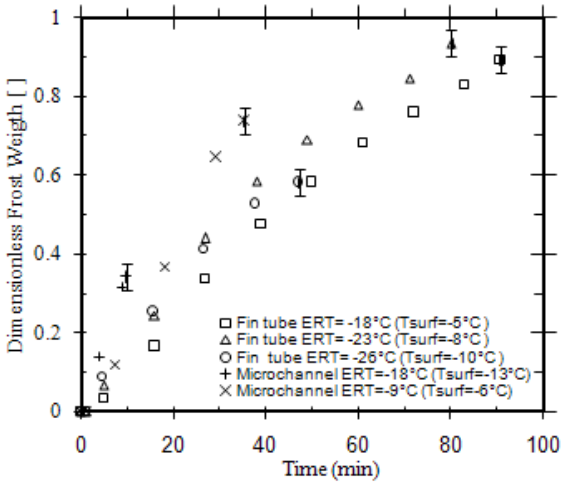

Figure 7: Comparison of frost weight between fin and tube and microchannel coil under same conditions

CONCLUSIONS

This paper presents a new technique to measure frost growth rate on heat exchangers. Images taken using a small tip CCD camera, mounted on a programmable robotic arm were used to measure the frost thickness in several locations of the coil. Data analysis from the current work indicated that air lift, drag, and friction effects on suspended coils could generate systematic errors in the frost weight measurements and a solution was proposed to eliminate these uncertainties. The experimental data showed that the onset of frost growth is strongly dependent on the local fin surface temperature and that the frost accumulated faster with air stream having higher vapour content. While the latter conclusion seems to be in agreement with previous studies, the effect from the fin surface temperature was isolated and highlighted in this study. The uneven fin temperature distribution, varying by distance form inlet header, caused the time lags of the onset of frost growth and different rate of frost accumulation. A microchannel coil, operating in similar working conditions, was also experimentally investigated and preliminary results indicated that it frosted faster than the fin and tube coil. The main reasons were attributed to its lower fin surface temperature and higher propensity of the fins to offer additional nucleation sites for frost growth.

ACKNOWLEDGMENTS

Authors would like to acknowledge the support from Oklahoma Centre for Advancement in Science & Technology (OCAST) and the Building Efficiency Group of Johnson Controls Inc.

REFERENCES

[1] J.-H. Kim and E. A. Groll, Microchannel Heat Exchanger Defrost Performance and Reliability, ASHRAE final report 1195-RP, Atlanta, GA, 2003.

[2] S. Padhmanabhan, D. E. Fisher, L. Cremaschi, and J. Knight, Comparison of Frost and Defrost Performance between Microchannel Coil and Fin-and-Tube Coil for Heat Pump Systems, in 12th Int. Refrigeration and Air Conditioning Conference at Purdue West Lafayette, IN, USA, paper no. R2202, 2008.

[3] D.-K. Yang, K.-S. Lee and S. Song, Modelling for Predicting Frosting Behavior of a Fin-Tube Heat Exchanger, International Journal of Heat and Mass Transfer, vol. 49, pp. 1472-1479, 2006.

[4] B. Na and R. L. Webb, Mass Transfer on and within a Frost Layer, Int. J. Heat Mass Tran., 47, 899-911, 2004.

[5] Y. Xia, P. S. Hrnjak, and A. M. Jacobi, Air-Side Thermal-Hydraulic Performance of Louvered-Fin, Flat-Tube Heat Exchangers with Sequential Frost-Growth Cycles, in ASHRAE Transactions, Orlando, FL, USA, vol. 111, pp. 487-495, 2005.

[6] K. Lenic, A. Trp and B. Frankovic, Transient Two-Dimensional Model of Frost Formation on a Fin-and-Tube Heat Exchanger, International Journal of Heat and Mass Transfer, vol. 52, pp. 22–32, 2009.

[7] A. Luer and H. Beer, Frost Deposition in a Parallel Plate Channel under Laminar Flow Conditions, International Journal of Thermal Science, vol. 39, pp. 85–95, 2000.

[8] H. Ohkubo, Advance of 'Study on Frosting Phenomena', Refrigeration, vol. 81, no. 942 pp. 255-9, 2006.

[9] J. Shin, A. V. Tikhonov and C. Kim, Experimental Study on Frost Structure on Surfaces With Different Hydrophilicity: Density and Thermal Conductivity, Journal of Heat Transfer, vol. 125, pp. 84-94, 2003.

[10] K.-S. Lee, W.-S. Kim and T.-H. Lee, One-Dimensional Model for Frost Formation on a Cold Flat Surface, Int. J. Heat and Mass Transfer, vol. 40, pp. 4359-4365, 1997.

[11] K.S. Lee, S. Jhee and D.K. Yang, Prediction of The Frost Formation on a Cold Flat Surface, Int. J. Heat Mass Transfer, vol. 46, pp. 3789–3796, 2003.

[12] B. Na, R. L. Webb, New Model for Frost Growth Rate, Int. J. Heat Mass Transfer, vol. 47, pp. 925–936, 2004.

[13] M. Fossa and G. Tanda, Frost Formation in Vertical Channels under Natural Convection, International Journal of Multiphase Flow, vol. 36 pp. 210–220, 2010.

[14] L. A. Kennedy and J. Goodman, Free Convection Heat and Mass Transfer under Conditions of Frost Deposition, International Journal of Heat and Mass Transfer, vol. 17, pp. 477-484, 1974.

[15] H. Chen, L. Thomas and R. W. Besant, Measurement of Frost Characteristics on Heat Exchanger Fins Part II: Data and Analysis, ASHRAE Transactions, vol. 105, Pt. 2, pp. 294-302, 1999.

[16] Y. Xia and A. M. Jacobi, Air-Side Data Interpretation and Performance Analysis for Heat Exchangers with Simultaneous Heat and Mass Transfer: Wet and Frosted Surfaces, Int. J. Heat Mass Transf., 48, 5089-102, 2005.

[17] T. Hosoda and H. Uzuhashi, Effects of Frost on the heat Transfer Coefficient, Hitachi Review, vol. 16, No. 6, pp. 254 -259, 1967.

[18] S. N. Kondepudi, The Effects of Frost Growth on Finned Tube Heat Exchangers under Laminar Flow, PhD Dissertation, Texas A&M University, TX, USA, 1988.

[19] S. Song, C.W. Bullard and P.S. Hanjak, Frost Deposition and Refrigerant Distribution in Microchannel Heat Exchangers, ASHRAE Trans., 108 (2), pp. 944–953.

[20] J. D. Yonko and C. F. Sepsy, An Investigation of the Thermal Conductivity of Frost while Forming on a Flat Horizontal Plate, ASHRAE Transactions, 73(2), pp. 2043-2053, 1967.

[21] P. Verma, D.M. Carlson, Y. Wu, P.S. Hrnjak, C.W. Bullard, Experimentally Validated Model for Frosting of Plain-Fin Round-Tube Heat Exchangers, International Conference of New Technologies in Commercial Refrigeration at University of Illinois at Urbana-Champaign, IL, USA, pp. 152-162, 2002.

[22] AHRI, AHRI Standard 210/240-2008, Performance Rating of Unitary Air Conditioning and Air-Source Heat Pump Equipment, AHRI, Ed. 2008.

[23] ASHRAE, ANSI/ASHRAE 41.2, Standard methods for laboratory airflow measurements, ASHRAE, Ed. 2001.

[24] S. Cai, Design of an Experimental Facility for Measurement of Frost Growth on Heat Exchangers, Master's Thesis, Oklahoma State University. 2009.

[25] C. Carroll and J. Peterson, Design and Construction of a Three-Axis Traverse System for an Image Capture in Frost Experiments, Senior Design Report, Oklahoma State University, OK, USA, 2009.

[26] S. Padhmanabhan, D. Fisher and L. Cremaschi, A Scaling Approach for Predicting Frost Growth in a Heat Exchanger – Application to Fin-Tube Coil, ASME-ATI-UIT 2010 Conference on Thermal and Environmental Issues in Energy Systems, May 2010, Sorrento, Italy. (in press)